

RESEARCH

Open Access



METTL16 accelerates lung adenocarcinoma progression by inducing N6-methyladenosine modification of GTSE1 to regulate p53 pathway and cell cycle

Fang Liu¹ and Sheng Jin^{2*}

Abstract

Background METTL16 has recently emerged as an N6-methyladenosine (m⁶A) methyltransferase that serves an integral role in tumor regulation. However, its involvement in lung adenocarcinoma (LUAD) remains unexamined. This investigation aims to explore METTL16's role and mechanism in LUAD progression.

Methods The expression of METTL16 and G2 and S phase-expressed-1 (GTSE1) in LUAD was evaluated by qRT-PCR or western blotting. LUAD cell malignancy was checked by CCK-8, wound healing, and transwell invasion assays. The relationship among METTL16 and GTSE1 was determined via Pearson correlation analysis and MeRIP assay. The p53 pathway-related proteins were detected by western blotting, and cell cycle was analyzed by flow cytometry.

Results METTL16 was elevated in LUAD, and its silencing significantly reduced LUAD cell proliferation, migration, and invasion. GTSE1 was significantly downregulated upon silencing METTL16. Furthermore, increased levels of GTSE1 mRNA and protein were found in LUAD, and it was correlated positively with METTL16 in LUAD tissues. The stability of GTSE1 was modulated by METTL16 in an m⁶A-dependent way, and GTSE1 overexpression partially rescued the suppressive effects METTL16 silencing on LUAD cells. In addition, GTSE1 overexpression also inhibited p53 pathway to promote LUAD cell cycle.

Conclusions These results indicate that METTL16-mediated m⁶A modification of GTSE1 accelerates LUAD progression by regulating p53 pathway and cell cycle. The aforementioned findings suggest METTL16 and GTSE1 may serve as potential targets for LUAD management.

Keywords METTL16, M⁶A modification, Lung adenocarcinoma, GTSE1, P53 pathway, Cell cycle

*Correspondence:

Sheng Jin

jinsheng13579@126.com

¹Department of Respiratory and Critical Care Medicine, Hubei No. 3, People's Hospital of Jiangnan University, No.26, Zhongshan Avenue, Qiaokou District, Wuhan 430033, Hubei, China

²Department of Nephrology, Rheumatology and Immunology, Hubei No. 3, People's Hospital of Jiangnan University, No.26, Zhongshan Avenue, Qiaokou District, Wuhan 430033, Hubei, China



© The Author(s) 2025. **Open Access** This article is licensed under a Creative Commons Attribution-NonCommercial-NoDerivatives 4.0 International License, which permits any non-commercial use, sharing, distribution and reproduction in any medium or format, as long as you give appropriate credit to the original author(s) and the source, provide a link to the Creative Commons licence, and indicate if you modified the licensed material. You do not have permission under this licence to share adapted material derived from this article or parts of it. The images or other third party material in this article are included in the article's Creative Commons licence, unless indicated otherwise in a credit line to the material. If material is not included in the article's Creative Commons licence and your intended use is not permitted by statutory regulation or exceeds the permitted use, you will need to obtain permission directly from the copyright holder. To view a copy of this licence, visit <http://creativecommons.org/licenses/by-nc-nd/4.0/>.

Introduction

Lung cancer is a widespread health issue, driving high mortality rates and imposing a significant economic and social burden [1]. In 2022, it was the most frequently diagnosed cancer, with around 2.48 million fresh cases and 1.82 million deaths, rendering it to be the leading contributor of cancer fatalities worldwide [2]. It has been categorized into non-small cell lung cancer (NSCLC) and small cell lung cancer (SCLC) types, with NSCLC making up about 85% of cases [3]. Lung adenocarcinoma (LUAD), a subtype of NSCLC, is characterized by rapid progression, distant metastasis, poor treatment response, and low survival rates [4, 5]. The survival rate for LUAD patients is below five years, and the cancer cells have been reported to rapidly acquire resistance to radiotherapy and chemotherapy after initial treatment [6, 7]. Hence, understanding the molecular mechanisms of LUAD progression is necessary for developing strategies for early diagnosis, effective treatment, and prognostic assessment.

The N⁶-methyladenosine (m⁶A) modification is the most common and crucial mRNA modification regulating pre-mRNA splicing, mRNA stability, mRNA decay, and translation, thus playing a vital part in normal physiology and disease conditions [8]. The m⁶A modification is a dynamic and reversible mechanism chiefly regulated via three types of catalytic enzymes, namely writers (“methyltransferases”), erasers (“demethylases”), and readers (“methylation-recognizing proteins”) [8]. Recently, METTL16 (methyltransferase-like 16 or METT10D), a member of the methyltransferase-like protein family, has gained attention for its function in adding m⁶A to various RNAs [9]. METTL16 features a Rossmann-like fold typical of methyltransferases of class I and utilizes S-adenosylmethionine for methyl donation, along with domains that are regulatory and RNA-binding [10]. It has been recognized as a potential candidate gene linked to the initiation and advancement of various cancers. Interestingly, its expression levels differ between distinct types of tumors and are associated with diverse clinical outcomes. For instance, a study identified significant alterations in METTL16 expression in hepatocellular carcinoma (HCC), demonstrating that increased expression of METTL16 was related to worse clinical outcomes [11]. Another study showed that METTL16 was highly present and correlated with poor survival outcomes in gastric cancer as it promoted tumor progression by increasing cyclin D1 expression via m⁶A methylation [12]. On the contrary, a study elucidated METTL16 as a potential biomarker and tumor suppressor in pancreatic ductal adenocarcinoma (PDA), showing that its low expression correlates with poor prognosis [13]. The findings imply that the role of METTL16 in cancer is complex and likely varies based on the type of cancer cells. Previously, only a

single study has reported that METTL16 expression was augmented in LUAD tissues in comparison to normal tissues, and promoted cell growth and migration [14]. However, the underlying molecular mechanisms by which METTL16 contributes to LUAD progression remain unexplored.

In the present research, we aimed to explore the role of METTL16 in LUAD and highlight the interaction between METTL16 and GTSE1 (G2 and S phase-expressed-1) involving in cell cycle and p53 pathway in LUAD cells. Using bioinformatic analysis and experiments, METTL16 upregulated in LUAD drives tumor progression by enhancing GTSE1 expression in an m⁶A-dependent manner to regulate p53 pathway and cell cycle. Our findings establish METTL16 as a pivotal oncogenic regulator in LUAD, acting through m⁶A-mediated GTSE1 mRNA modification to modulate p53 signaling and cell cycle.

Results

METTL16 was highly expressed in LUAD

The expression pattern of METTL16 in LUAD was checked by utilizing the mRNA expression dataset from the TNMplot database for comparing the expression profiles between LUAD tissues and adjoining non-tumor tissues. The results elucidated that METTL16 levels in LUAD tissues were notably higher as compared to normal tissues (Fig. 1A). The METTL16 mRNA expression in 46 LUAD and paired normal tissues was checked by qRT-PCR, and consistent to the observations of the TNMplot database analyses, the mRNA expression of METTL16 was elevated in LUAD tissues (Fig. 1B). In our collected LUAD cases, high expression of METTL16 was correlated with larger tumor size, advanced clinical stage, higher TNM stage, and metastasis (Table 1). Furthermore, we also determined METTL16 mRNA expression in four LUAD cell lines (A549, PC-9, H1373 and HCC4006), and found that it was markedly higher in them as compared to the BEAS-2B cell line (Fig. 1C). Due to the higher expression of METTL16 in A549 and PC-9 cell lines, the following experiments were performed in A549 and PC-9 cells.

METTL16 Silencing significantly suppressed the malignant phenotypes in LUAD cells via p53 pathway

We then explored the effect of METTL16 on LUAD cells in vitro by transfecting both the LUAD cell lines with two siRNAs that were specifically generated to target and silence METTL16 (si-METTL16#1 and si-METTL16#2). The outcomes of the qRT-PCR assay clearly showed the effective silencing of the relative expression of METTL16 (Fig. 2A). The CCK8 assay elucidated that the cell proliferation was significantly diminished upon silencing METTL16 (Fig. 2B). The wound healing assay further

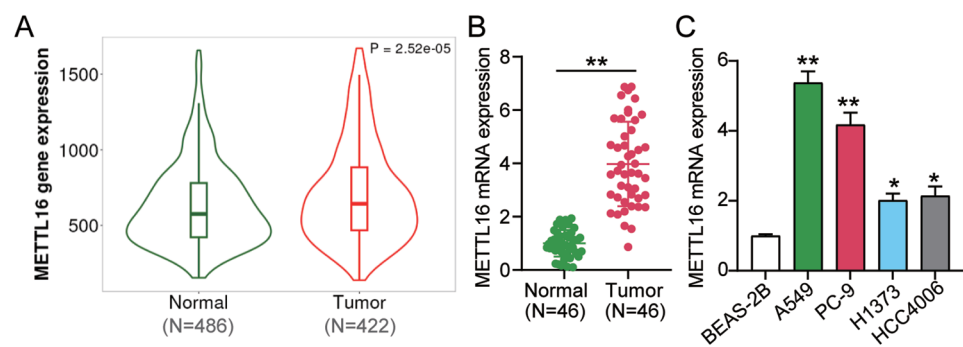


Fig. 1 Increased METTL16 expression was found in LUAD, as determined by TNMplot database and qRT-PCR. **(A)** The METTL16 gene expression in LUAD and healthy normal tissues according to the data from TNMplot database. **(B)** The mRNA expression of METTL16 in LUAD tissues ($n = 46$) and adjacent normal tissues ($n = 46$) was detected by qRT-PCR. [$**P < 0.001$ vs. normal tissues]. **(C)** The mRNA expression of METTL16 in both the LUAD cell lines (A549, PC-9, H1373 and HCC4006) and normal lung epithelial cell line BEAS-2B was detected by qRT-PCR. [$**P < 0.001$ vs. BEAS-2B]

Table 1 The correlation between METTL16/GTSE1 expression and clinical features

Characteristics	METTL16 expression		P-value	GTSE1 expression		P-value
	High (n = 21)	Low (n = 25)		High (n = 25)	Low (n = 21)	
Sex			> 0.9999			0.3672
Male	13	15		17	11	
Female	8	10		8	10	
Age (years)			0.3721			0.7664
<60	11	9		10	10	
≥60	10	16		15	11	
Tumor size (cm)			0.0028			0.0229
<3	1	11		3	9	
≥3	20	14		22	12	
Clinical stage			0.0039			0.0009
I/II	14	23		12	20	
III/IV	12	2		13	1	
TNM stage			0.0027			0.0132
1/2	12	24		16	20	
3/4	9	1		9	1	
Lymph node metastasis			< 0.0001			0.0006
No	6	23		10	19	
Yes	15	2		15	2	

demonstrated that the METTL16 silencing markedly suppressed the migrative potentials of LUAD cells (Fig. 2C). The transwell invasion assay illustrated that silencing of METTL16 notably repressed the invasion of LUAD cells (Fig. 2D). Moreover, western blotting found that METTL16 silencing elevated phosphorylated p53 (p-p53) levels (Fig. 2E). Altogether, the aforementioned results imply that METTL16 downregulation hinders the advancement of LUAD by repressing cell proliferation, migration, and invasion via activating p53 pathway.

Six genes May affect LUAD progression through p53 signaling pathway and cell cycle

We utilized the Venny 2.1 tool to determine overlapping genes between the upregulated DEGs and survival-related genes from the GEPIA-LUAD database, resulting in 101 common genes (Fig. 3A). GO enrichment analysis

of these 101 common genes identified the cell cycle as a key biological process (Fig. 3B). Similarly, KEGG enrichment analysis highlighted the p53 signaling pathway as the central signaling pathway associated with these genes (Fig. 3C). Finally, again by utilizing Venny 2.1, used to overlap the common genes associated with cell cycle and p53 signaling pathway. Finally, once again utilizing Venny 2.1, the common genes overlapping between the aforementioned two pathways were identified, revealing six common genes (Fig. 3D). These genes were CCNB1, CDK1, CHEK1, RRM2, CCNB2, and GTSE1. Therefore, we speculated that METTL16 may influence LUAD progression by regulating these key genes involved in the p53 signaling pathway and cell cycle.

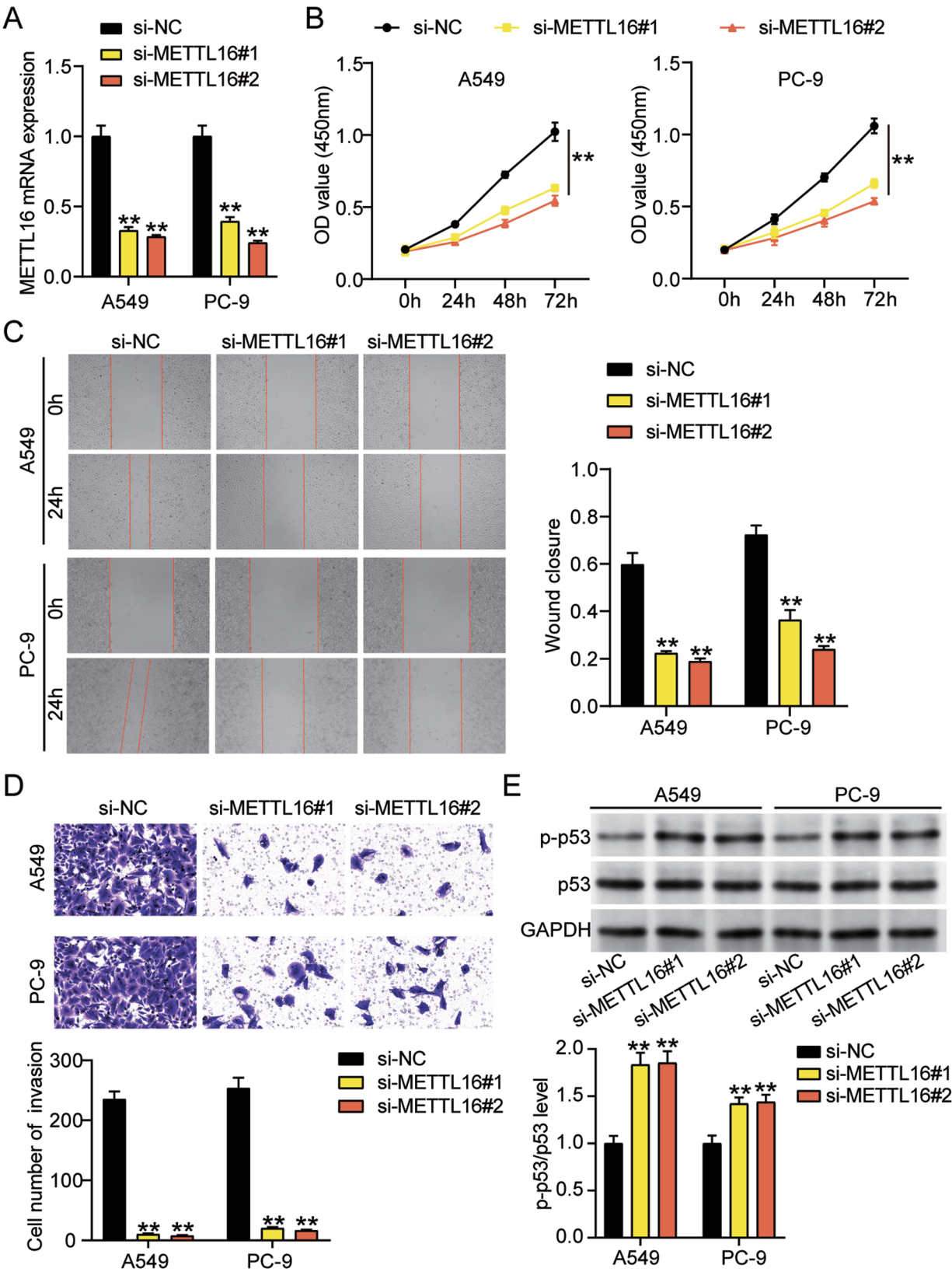


Fig. 2 (See legend on next page.)

(See figure on previous page.)

Fig. 2 METTL16 silencing reduced LUAD cell proliferation, migration, and invasion via p53 pathway, as verified by qRT-PCR, cell functional experiments, and western blotting. **(A)** The transfection efficiency of silencing METTL16 (si-METTL16#1 and si-METTL16#2) in A549 and PC-9 cell lines was detected by qRT-PCR. **(B)** The effect of METTL16 silencing on the proliferation of LUAD cells was checked by CCK8 assay. **(C)** The effect on the migration of LUAD cells post METTL16 silencing was evaluated by wound healing assay. **(D)** The invasion of LUAD cells was evaluated by transwell invasion assay after silencing METTL16. **(E)** Western blotting detected the protein expression of phosphorylated p53 (p-p53) and p53 in LUAD cells with the transfection of si-METTL16#1 and si-METTL16#2. [$^{*}P < 0.001$ vs. si-NC]

METTL16 targeted GTSE1 by regulating its m⁶A modification

We next screened the aforementioned six common genes overlapping between the cell cycle and the p53 pathway by analyzing their mRNA expression in LUAD cells following METTL16 silencing. The qRT-PCR assay results showed that, out of the six genes, only GTSE1 was significantly downregulated following METTL16 silencing in both LUAD cell lines (Fig. 4A). Similar to the observed mRNA changes, the protein expression of GTSE1 was also notably reduced upon METTL16 silencing (Fig. 4B). We then observed that the GTSE1 mRNA levels were increased in our collected LUAD tissues as compared to the neighboring non-tumor tissues (Fig. 4C). Meanwhile, high expression of GTSE1 was correlated to larger tumor size, advanced clinical stage, higher TNM stage, and metastasis (Table 1). Moreover, the expressions of METTL16 and GTSE1 demonstrated a positive correlation with each other (Fig. 4D). The Me-RIP assay demonstrated that GTSE1 was significantly enriched by anti-m⁶A, but METTL16 silencing in LUAD cells significantly reduced the enrichment of GTSE1 (Fig. 4E). In addition, GTSE1 knockdown could not affect METTL16 expression (Supplementary Fig. 2), suggesting that GTSE1 was a downstream of METTL16. The results clearly suggest that GTSE1 as the downstream of METTL16 can be positively modulated via mediating its m⁶A modification.

GTSE1 knockdown reduced LUAD cell proliferation, migration, and invasion

After transfecting LUAD cells with si-GTSE1#1 and si-GTSE1#2, qRT-PCR assay showed the effective silencing of the relative expression of GTSE1 (Supplementary Fig. 1A). The CCK8 assay elucidated that silencing GTSE1 inhibited the cell proliferation (Supplementary Fig. 1B). The data of wound healing assay demonstrated that the GTSE1 knockdown markedly suppressed the migrative potentials of LUAD cells (Supplementary Fig. 1C). The transwell invasion assay illustrated that silencing GTSE1 notably impaired LUAD cell invasion (Supplementary Fig. 1D). All results imply that GTSE1 downregulation hinders LUAD cell proliferation, migration, and invasion.

METTL16 interacted with GTSE1 to affect LUAD progression in vitro

Finally, we conducted in vitro rescue experiments to investigate the interactions between METTL16 and GTSE1 in the progression of LUAD. We transfected GTSE1 overexpression vector (OE-GTSE1) or negative control (OE-NC) into METTL16 silenced cells for rescue experiments. We conducted the rescue experiments using only one METTL16 siRNA, selecting the second siRNA due to its more pronounced effect (see Fig. 2). The outcomes of the CCK8 assay elucidated that GTSE1 overexpression significantly counteracted the suppressive effects of METTL16 silencing on the proliferative properties of LUAD cells (Fig. 5A). Wound healing assay also elucidated that GTSE1 overexpression partly attenuated the METTL16-silencing-induced repression of the migrative abilities of LUAD cells (Fig. 5B). Similarly, the transwell invasion assay unfolded that GTSE1 overexpression markedly reversed the inhibitory effect of METTL16 silencing on the invasive capabilities of LUAD cells (Fig. 5C). These outcomes illustrate that METTL16 influences the progression of LUAD by interacting with and regulating the expression of GTSE1.

GTSE1 knockdown induced cell cycle arrest at S phase via p53 pathway

To further confirm the bioinformatic analysis results in Fig. 3, western blotting found that GTSE1 knockdown reduced GTSE1 levels and elevated phosphorylated p53 (p-p53) levels, whereas GTSE1 overexpression enhanced GTSE1 levels and declined p-p53 levels in LUAD cells (Fig. 6A). In addition, flow cytometry analysis showed that GTSE1 knockdown raised the cell percentage of S phase, but GTSE1 overexpression reduced the cell percentage of S phase (Fig. 6B). All data prove that GTSE1 knockdown induces cell cycle arrest at S phase via activating p53 pathway.

Discussion

Given the emerging importance of m⁶A modification in cancer biology, we looked into the role of METTL16 (m⁶A methyltransferase) in LUAD. In this present work, it was found that METTL16 was upregulated in LUAD, and its silencing reduced the malignant properties of LUAD cells in vitro. Furthermore, we showed that METTL16 enhanced the progression of LUAD via regulating the expression of GTSE1 by mediating its m⁶A

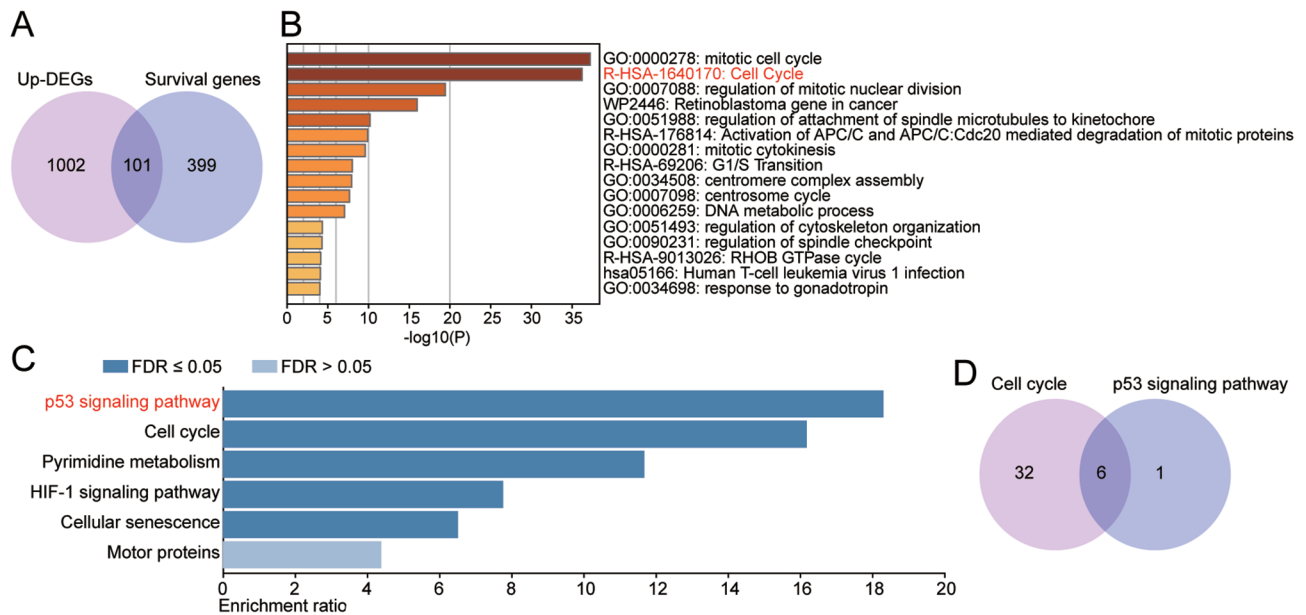


Fig. 3 Six genes may affect LUAD progression through p53 signaling pathway and cell cycle, as predicted by bioinformatic analysis. **(A)** Venny 2.1 tool was used to overlap the common genes from upregulated differentially expressed genes (DEGs) and survival genes from GEPIA-LUAD database. **(B)** The Gene Ontology (GO) enrichment was done on the 101 common genes to select the key biological process by Metascape. **(C)** The Kyoto Encyclopedia of Genes and Genomes (KEGG) enrichment was performed on 101 common genes to select the key signaling pathway by WebGestalt. **(D)** Venny 2.1 tool was used to overlap the common genes associated with cell cycle and p53 signaling pathway

modification to regulate p53 pathway and cell cycle. Additionally, we demonstrated that METTL16 facilitated the progression of LUAD by modulating GTSE1 expression through m⁶A modification, thereby impacting the p53 pathway and cell cycle (Fig. 7).

Current evidence suggests that the METTL3-METTL14 methyltransferase complex is primarily responsible for depositing m⁶A modifications on mRNA [8]. However, METTL3 and METTL14 are responsible for approximately 60% of m⁶A modifications in certain types of cells, with many m⁶A sites not aligning closely with the binding regions of these two, suggesting the existence of another m⁶A methyltransferase at play [15]. METTL16 is a recently discovered methyltransferase capable of independently adding the m⁶A modification, although its functions remain not fully understood [16]. Several previous reports have highlighted a connection between METTL16 and different cancers, where it may either promote tumor initiation or act as a suppressor. Previously, elevated METTL16 expression has been linked to tumor progression in HCC and gastric cancer [11, 12]. Additionally, bioinformatics analyses have also revealed its overexpression and association with poor survival outcomes in HCC, colorectal cancer (CRC), glioma, endocrine tumors, soft-tissue sarcomas, melanoma, and breast cancer [17]. Herein, we observed that METTL16 was highly expressed in LUAD tissues and cell lines. Furthermore, its silencing notably reduced the malignant phenotypes of LUAD cell lines. This study

innovatively revealed the upregulation of METTL16 in LUAD and suggest that it may play an oncogenic role in LUAD tumorigenesis.

Our bioinformatics analysis identified GTSE1 as a target of METTL16 in LUAD, with METTL16 modulating GTSE1 stability through m⁶A methylation. GTSE1 is located on chromosome 22q13.2-q13.3 and is primarily expressed during the G2 and S stages of the cell cycle [18]. It has been shown to contribute to tumor progression by inhibiting p53-induced apoptosis and acting as a negative regulator of p53, promoting its nuclear export and degradation [19]. Consistent with previous studies, this study also confirmed that GTSE1 could inhibit p53 signaling pathway to promote cell cycle progression in LUAD cells. In addition, recent investigations have shown that GTSE1 expression is increased in various tumors. For instance, high GTSE1 has been linked to renal cell carcinoma and closely linked with poor prognostic clinicopathological features [20]. It has been shown to be overexpressed in esophageal squamous cell carcinoma (ESCC) and promoted chromosomal instability, oxidative stress, and JNK pathway activation, inhibiting apoptosis thereby driving ESCC tumorigenesis [21]. Elevated GTSE1 expression has also been detected in osteosarcoma tissues and cell lines [22]. It was also elevated and promoted breast cancer progression, metastasis, multidrug resistance, and poor prognosis, especially in p53-mutated cases [23]. Moreover, various bioinformatics studies have also shown elevated expression of

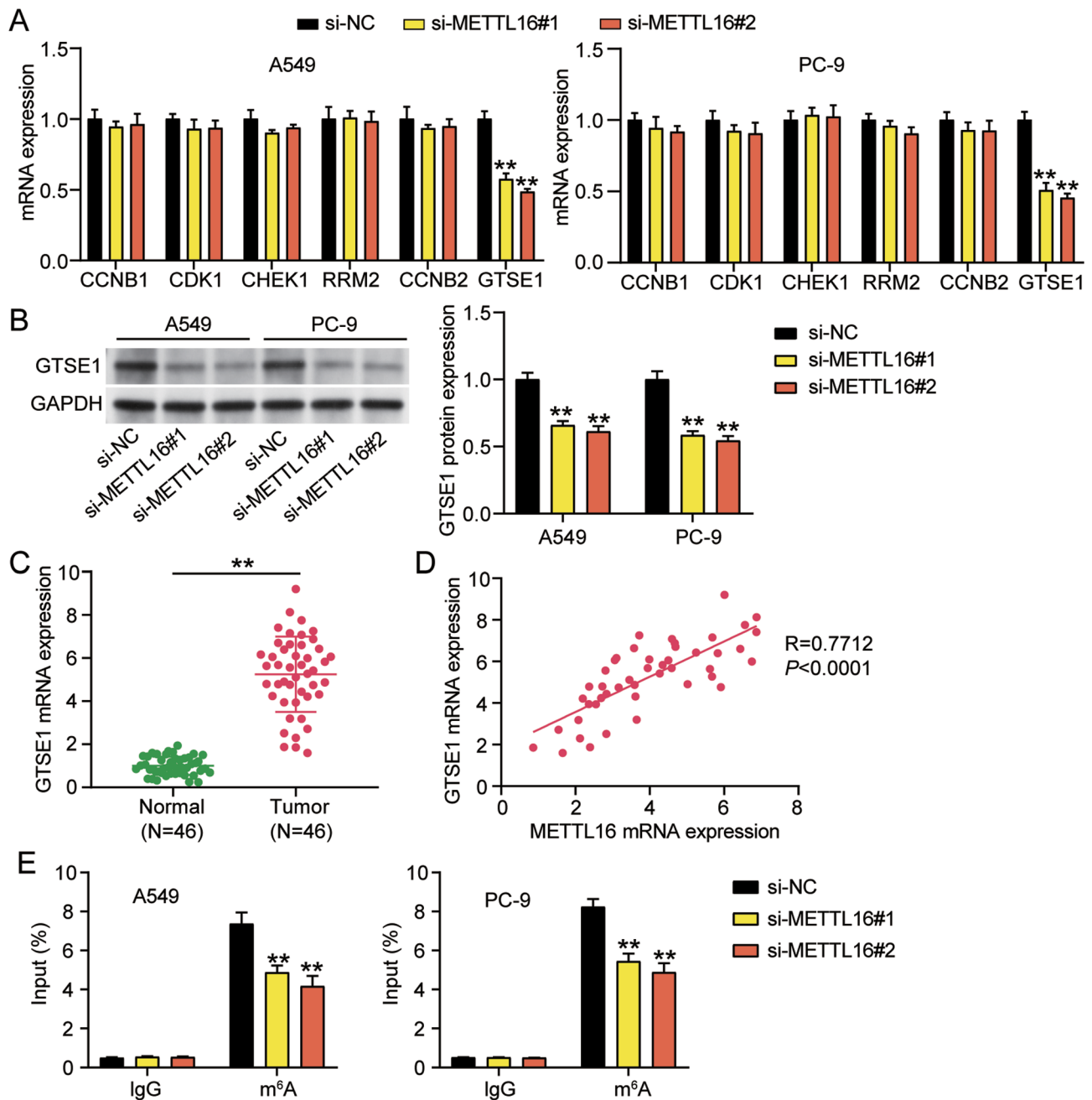


Fig. 4 METTL16 regulates GTSE1 stability via m⁶A modification, as demonstrated by MeRIP and qRT-PCR. The mRNA expression of six common genes (CCNB1, CDK1, CHEK1, RRM2, CCNB2, GTSE1) in LUAD cell lines after METTL16 silencing was determined by qRT-PCR. [^{**} $P < 0.001$ vs. si-NC]. (B) The protein expression of GTSE1 in LUAD cell lines after METTL16 silencing was evaluated by Western blotting. [^{**} $P < 0.001$ vs. si-NC]. (C) The expression of GTSE1 in LUAD tissues ($n = 46$) and adjacent normal tissues ($n = 46$) was detected by qRT-PCR. [^{**} $P < 0.001$ vs. normal tissues]. (D) Correlation between the expression of METTL16 and GTSE1 in LUAD tissues was assessed by Pearson correlation analysis. (E) The m⁶A modification of GTSE1 was determined by MeRIP assay. [^{**} $P < 0.001$ vs. anti-IgG]

GTSE1 in wide range of tumor tissues, including LUAD [24–26]. We innovatively revealed the elevated expression of GTSE1 in LUAD tissues to the best of our knowledge. Furthermore, we showed that METTL16 promotes LUAD progression by enhancing the expression of GTSE1 by mediating its m⁶A modification, highlighting

the interaction between METTL16 and GTSE1 as one of the key mechanisms driving LUAD progression.

The current work has certain limitations that warrant further examination. First, while the findings primarily rely on in vitro experiments, future research is needed to validate these results in vivo to enhance their

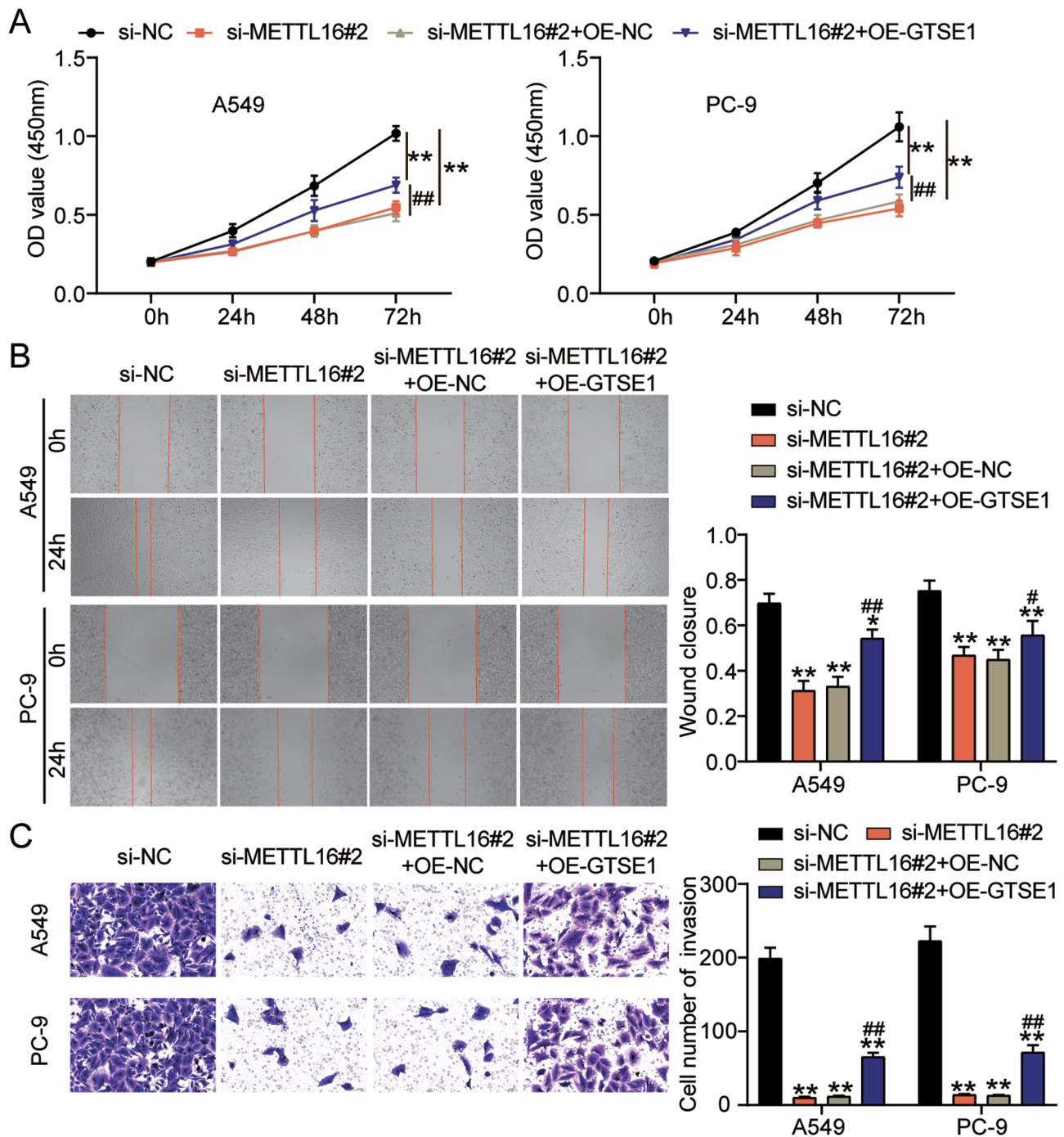


Fig. 5 METTL16 interacted with GTSE1 to influence the progression of LUAD in vitro, as detected by cell functional experiments. The LUAD cells were transfected with GTSE1 overexpression vector (OE-GTSE1) or negative control (OE-NC) into METTL16 silenced (si-METTL16#2) cells for rescue experiments (A) The cell proliferation in the aforementioned transfected LUAD cells was assessed by means of the CCK-8 assay. (B) The cell migration in the aforementioned transfected LUAD cells was evaluated by wound healing assay. (C) The invasion of LUAD cells following the aforementioned transfections was evaluated by means of the transwell invasion assay. [$*P < 0.05$, $**P < 0.001$ vs. si-NC and $##P < 0.001$ vs. si-METTL16#2 + OE-NC]

relevance and applicability. Second, the limited number of tissue samples analyzed may constrain the broader applicability of the conclusions. Next, although the study focused on interactions of METTL16 and GTSE1 in LUAD, there may be additional pathways through

which METTL16 influences the overall disease progression. Exploring these alternative mechanisms in greater detail will give a more comprehensive picture. Moreover, oncogenic driver mutations may modulate the function of METTL16 and its downstream target GTSE1. Our

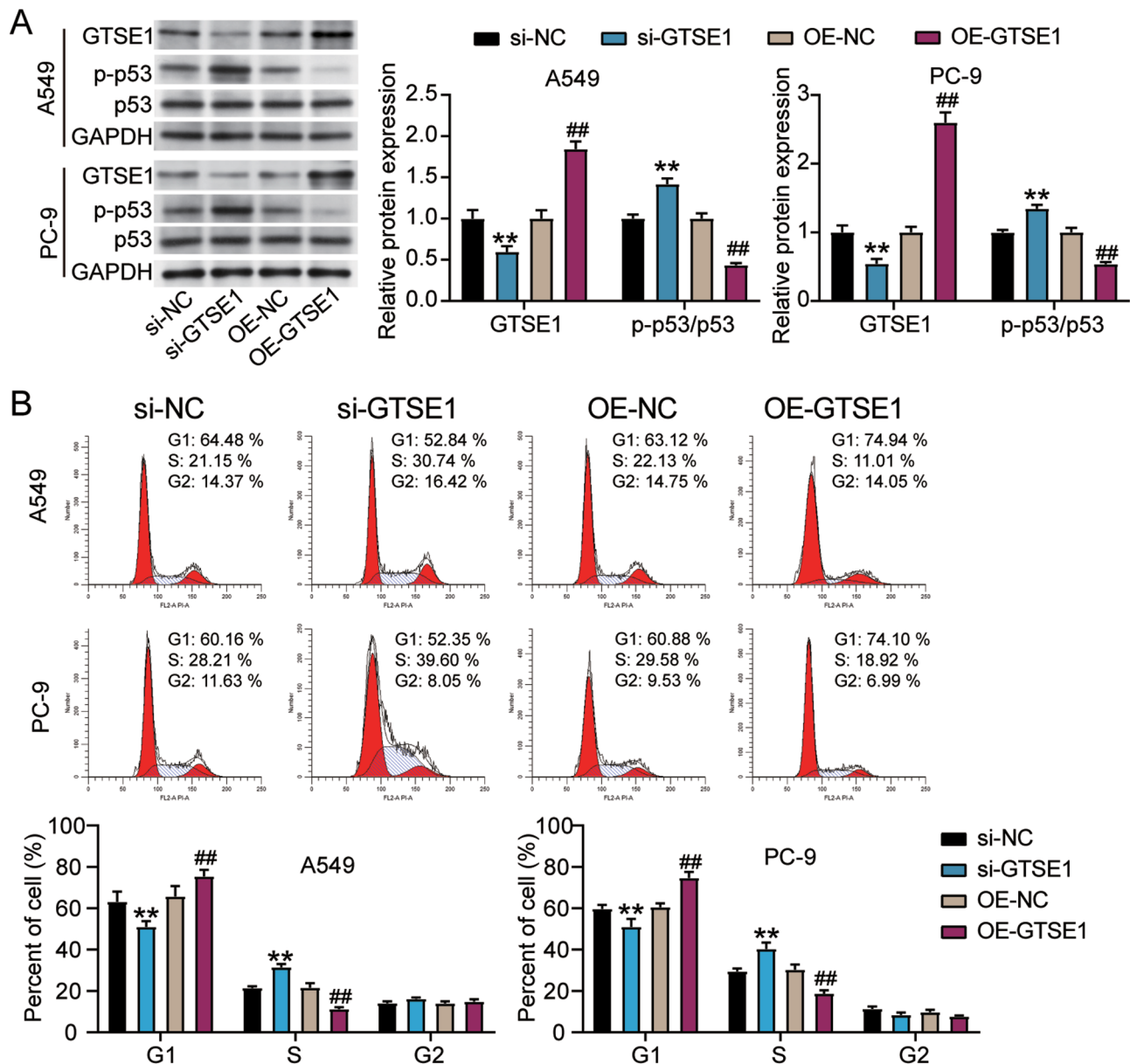


Fig. 6 GTSE1 knockdown activated p53 pathway to induce cell cycle arrest, as verified by western blotting and flow cytometry. **(A)** Western blotting detected the protein expression of GTSE1, phosphorylated p53 (p-p53) and p53 in LUAD cells with the transfection of GTSE1 knockdown or GTSE1 over-expression vectors. **(B)** Flow cytometry measured cell cycle in LUAD with the transfection of GTSE1 knockdown or GTSE1 overexpression vectors. [$**P < 0.001$ vs. si-NC and $##P < 0.001$ vs. OE-NC]

current study observed METTL16-dependent effects on GTSE1 expression, p53 signaling, and cell cycle progression in A549 and PC9 cell lines. This suggests that METTL16's oncogenic role in LUAD may transcend specific oncogenic driver mutations (KRAS, EGFR and TP53). Future research in additional models (e.g., EGFR/KRAS/TP53 isogenic cell lines) should be performed to clarify whether METTL16's effects are universally conserved or mutation-subtype-dependent.

Overall, our results elucidated that METTL16 was upregulated in LUAD and its silencing reduced the

malignant properties of LUAD cells. Furthermore, METTL16 promoted the advancement of LUAD by mediating the m⁶A modification of GTSE1 to regulate p53 pathway and cell cycle. These findings contribute to understanding the molecular mechanisms involving METTL16 and its role in m⁶A modification, highlighting their potential diagnostic and therapeutic significance in LUAD.

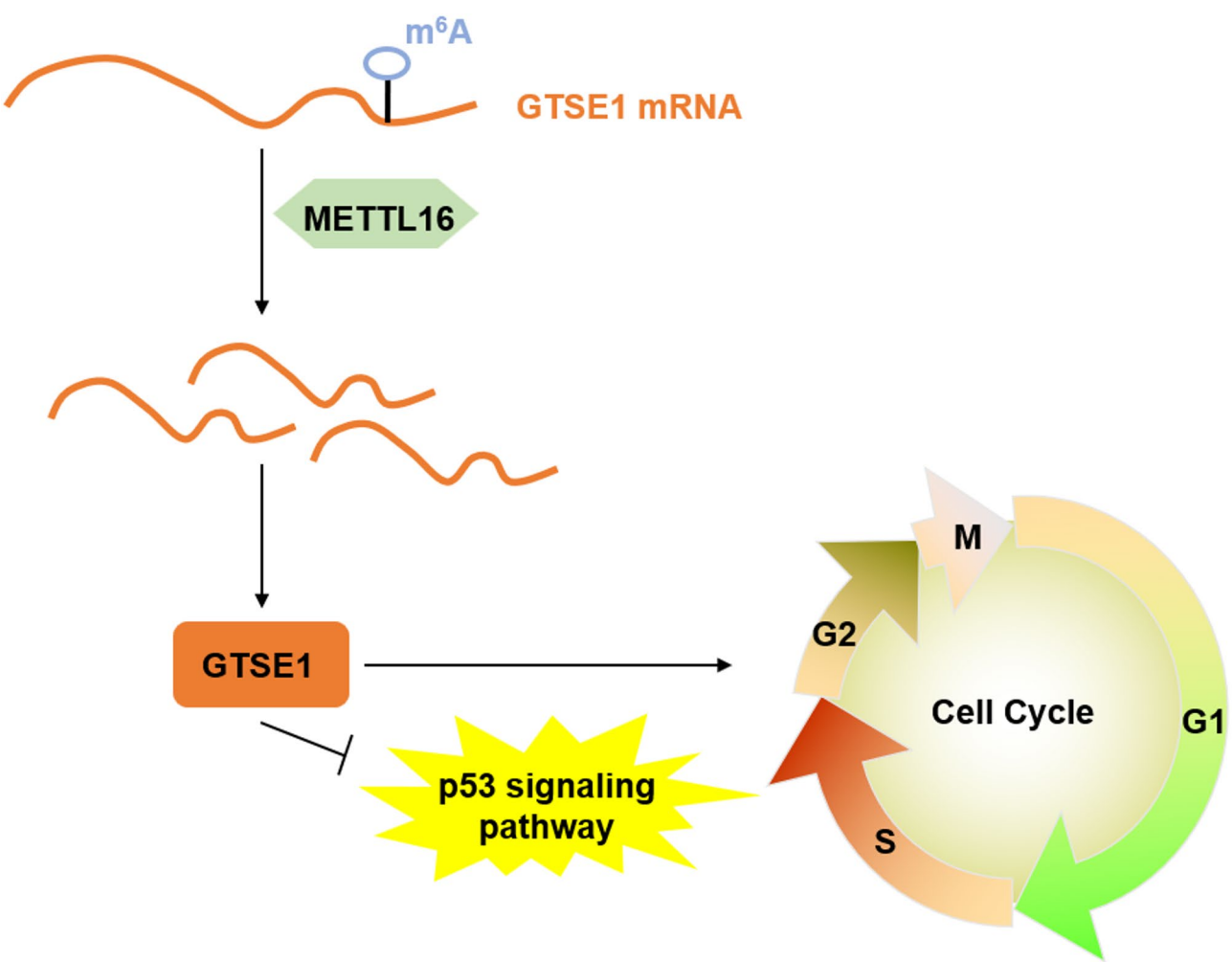


Fig. 7 A schematic diagram illustrating our findings on METTL16-mediated m⁶A modification of GTSE1 in LUAD

Table 2 Clinical features of lung adenocarcinoma patients (N= 46)

Characteristics	Patients (N)	Percentage (%)
Sex		
Male	28	39.1
Female	18	60.9
Age (years)		
<60	20	43.5
≥60	26	56.5
Tumor size (cm)		
<3	12	26.1
≥3	34	73.9
Clinical stage		
I/II	32	69.6
III/IV	14	30.4
TNM stage		
1/2	36	78.3
3/4	10	21.7
Lymph node metastasis		
No	29	63.0
Yes	17	37.0

Materials and methods

Clinical specimens

The ethics committee of Hubei No.3 People’s Hospital of Jiangnan University approved this research (IRB: 2023-012). LUAD and the corresponding adjoining non-tumor tissues were acquired by means of surgery from 46 LUAD patients registered in our hospital. The patients had not received any treatments prior to admission and were diagnosed with LUAD through histological examination. The clinical characteristics are tabulated in Table 2. All the patients signed the written informed consent prior to the investigation.

Cell culture and transfections

The four LUAD cell lines including A549 (CL-001 h), PC-9 (CL-013 h), H1373 (CL-070 h) and HCC4006 (CL-587 h), as well as the normal lung epithelial cell line BEAS-2B (CL-016 h) were purchased from Wuhan SAIOS (China). The cell lines were cultured using the following media: A549 cells in F-12 K medium (Wuhan

Table 3 Primer sequence used in qRT-PCR

Gene	Sequence (5'–3')
METTL16	F: CTCTGACGTGTACTCTCCTAAGG R: TACCAGCCATTCAAGGTTGCT
CCNB1	F: CTTAGACAAATTCTGAAGTAGTGATA R: ATTCTTGACAACGGTGAAT
CDK1	F: AAAGCTACAGGTCAGTGGTAGCC R: TCCTGCATAAGCACATCTCTGA
CHEK1	F: GGTACAGGAGAGAAGGAAT R: TCTCTGACCATCTGGTTCAGG
CCNB2	F: AAAGCTCAGAACACCAAGTTCCA R: ACAGAAGCAGTAGGTTTCAGTTGT
RRM2	F: TTACATAAAAGATCCCAAGAAAGG R: AGCCTCTTTGTCCCAATC
GTSE1	F: CAGGGGACGTGAACATGGATG R: ATGTCCAAAGGTCGAAGAA
GAPDH	F: GGAGCGAGATCCCTCCAAAT R: GGCTGTTGTCATCTTCTCATGG

SAIOS); H1373, HCC4006 and PC-9 cells in RPMI-1640 medium (Wuhan SAIOS); and BEAS-2B cells in DMEM medium (Wuhan SAIOS). All cells were cultured by adding 10% FBS (Wuhan SAIOS), and incubated under the condition of 5% CO₂ and 37°C.

Two METTL16-targeting small interfering RNAs (si-METTL16#1 and si-METTL16#2) and the negative control (si-NC) were ordered from RiboBio, China. The overexpression vector of GTSE1 (OE-GTSE1) was also constructed by RiboBio using the pcDNA3.1 vector, while the empty vector of pcDNA3.1 was a negative control (OE-NC). Additionally, Lipofectamine 3000 (Thermo Fisher Scientific, USA) was utilized for cell transfections and the transfection efficiency was checked 48-hour post-transfection via qRT-PCR.

RNA extractions and quantitative real time PCR (qRT-PCR)

The total RNA was extracted from LUAD tissues and cell lines (A549 and PC-9) via Trizol method by means of the Trizol reagent (Invitrogen, USA). Next, cDNA was generated by utilizing Evo m-mlv reverse transcription reagent (Accurate Biology, Changsha, China). Then, qRT-PCR was conducted using SYBR green pro kit (Accurate Biology). The data were quantitatively analyzed via the 2^{−ΔΔCt} method, and GAPDH was used as the internal control. The primer sequences are presented in Table 3.

Cell counting Kit-8 (CCK-8) assay

The LUAD cells (3000 cells/well) were inoculated onto 96-well plates and incubated for 0, 24, 48, and 72 h. At the end of the specified duration, 10 μL of CCK-8 reagent (Beyotime, China) was put into each well, and a 2-hour incubation was carried out at 37 °C. Lastly, the absorbance was taken by employing a microplate reader (Hiwell Diatek, Wuxi, China) at 450 nm.

Wound healing assay

The LUAD cells were grown in 6-well plates until they reached 95% confluence. Next, the cell monolayer was scraped with a micropipette tip to create a wound. The detached/damaged cells were removed with PBS, and the remaining cells were cultivated in a serum free media for 24 h at 37 °C. The wounds were analyzed and imaged at 0 and 24 h using an inverted microscope, and the wound areas at both the time points were quantified.

Transwell invasion assay

Millipore transwell inserts (USA) in a 24-well plate were employed for this assay. Firstly, the upper transwell chamber was precoated with 8% Matrigel. Following this, 600 μL of culture media supplemented with 20% FBS (chemoattractant) was put in the bottom chamber, while LUAD cells (1 × 10⁵) suspended in 200 μL of serum free culture media were put in the upper chamber. Following a 12-hour incubation at 37 °C, those cells that invaded the bottom surface of inserts were fixed with paraformaldehyde (4%), stained with crystal violet (0.1%), and counted using microscopy.

Bioinformatics analysis

The TNMplot database (<https://tnmplot.com/analysis/>) was employed to analyze the expression level of METTL16 in LUAD samples. Additionally, the Venny 2.1 tool was used to determine overlapping genes between upregulated differentially expressed genes (DEGs) screened by log2 FC > 1 and adj.P < 0.01, and survival-associated genes screened by P < 0.01 from the GEPIA-LUAD database. Furthermore, Gene Ontology (GO) of these overlapping genes was analyzed via Metascape, and Kyoto Encyclopedia of Genes and Genomes (KEGG) enrichment of these overlapping genes was analyzed via WebGestalt.

Western blotting

The LUAD cells were treated with a RIPA lysis buffer (BOSTER, Wuhan, China) to extract their total proteins and the concentration was evaluated via a BCA Protein Assay Kit (Beyotime, China). Next, the proteins were separated by performing SDS-PAGE before being transferred onto PVDF membranes. These membranes were then blocked with 5% skimmed milk and then treated with primary antibodies (*anti-GTSE1*: A13903, ABclonal Biotechnology, China, *anti-p53*: A25915, ABclonal Biotechnology, China, *anti-phospho-p53*: AP0083, ABclonal Biotechnology, China, and *anti-GAPDH*: AC027, ABclonal Biotechnology, China) overnight at 4 °C. On the following day, these membranes were treated with the secondary antibody (HRP-labeled) raised in goat for 1 h at room temperature, and the bands of protein were

observed with the help of BeyoECL Plus (Beyotime, China).

Methylated RNA Immunoprecipitation (Me-RIP) assay

The assay was done by employing Magna RIP™ RNA-Binding Protein Immunoprecipitation kit (Millipore Sigma, USA). The RNAs of LUAD cells stably transfected with either si-METTL3 or si-NC were extracted. Thereafter, RNAs were sheared into fragments by treating with Fragmentation Reagents. Following that, immunoprecipitations were performed by incubating the fragmented RNAs with the magnetic beads conjugated with either anti-IgG or anti-m6A antibodies in the IP buffer. Then the RNAs were eluted from the beads following a 1-hour incubation with elution buffer at 4 °C. Both input and eluted RNAs were harvested following precipitation, converted into cDNA through reverse transcription, and analyzed by qRT-PCR.

Cell cycle detection

Flow cytometry (Beckman, USA) was used to detect cell cycle using Cell Cycle and Apoptosis Analysis Kit (Beyotime, China). LUAD cells (1×10^6) were firstly fixed in pre-cooling 70% ethanol for 12 h at 4 °C. LUAD cells were stained with 0.5 mL PI staining solution for 30 min at 37 °C without light, and immediately detected cell cycle using flow cytometry.

Statistical analysis

The data analyses were done in Graphpad Prism statistical software. All the data were indicated as the mean \pm standard deviation. The comparisons between two groups and more than two groups were accomplished by Student's t-test and one-way ANOVA (with Tukey's post-hoc), respectively. The correlation among METTL16 and GTSE1 was determined using Pearson correlation analysis. P values less than 0.05 were indicative of statistical significance.

Supplementary Information

The online version contains supplementary material available at <https://doi.org/10.1186/s13008-025-00156-y>.

Supplementary Material 1

Supplementary Material 2

Acknowledgements

None.

Author contributions

Fang Liu designed this research, executed the experiments and wrote original manuscript. Sheng Jin performed data analysis and reviewed this manuscript. All authors read and approved this manuscript.

Funding

None.

Data availability

The datasets produced and/or utilized in this study are available from the corresponding author upon reasonable request.

Declarations

Conflict of interest

The authors have no conflicts of interest to disclose.

Ethics approval

The study received approval from the Ethics Committee of Hubei No.3 People's Hospital of Jiangnan University. All clinical samples were handled in full compliance with the ethical standards outlined in the Declaration of Helsinki. Written informed consent was obtained from all patients involved in the study.

Received: 22 January 2025 / Accepted: 8 May 2025

Published online: 22 May 2025

References

1. Yousefi M, Jalilian H, Heydari S, Seyednejad F, Mir N. Cost of lung cancer: A systematic review. *Value Health Reg Issues*. 2023;33:17–26.
2. Bray F, Laversanne M, Sung H, Ferlay J, Siegel RL, Soerjomataram I, et al. Global cancer statistics 2022: GLOBOCAN estimates of incidence and mortality worldwide for 36 cancers in 185 countries. *CA Cancer J Clin*. 2024;74(3):229–63.
3. Inamura K. Lung cancer: Understanding its molecular pathology and the 2015 WHO classification. *Front Oncol*. 2017;7:193.
4. Tian S. Classification and survival prediction for early-stage lung adenocarcinoma and squamous cell carcinoma patients. *Oncol Lett*. 2017;14(5):5464–70.
5. Wang H, Han G, Chen J. Heterogeneity of tumor immune microenvironment in malignant and metastatic change in LUAD is revealed by single-cell RNA sequencing. *Aging*. 2023;15(12):5339–54.
6. Yu H, Zhang W, Xu XR, Chen S. Drug resistance related genes in lung adenocarcinoma predict patient prognosis and influence the tumor microenvironment. *Sci Rep*. 2023;13(1):9682.
7. Min W, Sun L, Li B, Gao X, Zhang S, Zhao Y. LncCRLA enhanced chemoresistance in lung adenocarcinoma that underwent epithelial-mesenchymal transition. *Oncol Res*. 2022;28(9):857–72.
8. Hong J, Xu K, Lee JH. Biological roles of the RNA m(6A) modification and its implications in cancer. *Exp Mol Med*. 2022;54(11):1822–32.
9. Warda AS, Kretschmer J, Hackert P, Lenz C, Urlaub H, Hobartner C, et al. Human METTL16 is a N(6)-methyladenosine (m(6A)) methyltransferase that targets pre-mRNAs and various non-coding RNAs. *EMBO Rep*. 2017;18(11):2004–14.
10. Satterwhite ER, Mansfield KD. RNA methyltransferase METTL16: targets and function. *Wiley Interdiscip Rev RNA*. 2022;13(2):e1681.
11. Wang P, Wang X, Zheng L, Zhuang C. Gene signatures and prognostic values of m6A regulators in hepatocellular carcinoma. *Front Genet*. 2020;11:540186.
12. Wang XK, Zhang YW, Wang CM, Li B, Zhang TZ, Zhou WJ, et al. METTL16 promotes cell proliferation by up-regulating Cyclin D1 expression in gastric cancer. *J Cell Mol Med*. 2021;25(14):6602–17.
13. Lu L, Zheng D, Qu J, Zhuang Y, Peng J, Lan S, et al. METTL16 predicts a favorable outcome and primes antitumor immunity in pancreatic ductal adenocarcinoma. *Front Cell Dev Biol*. 2022;10:759020.
14. Wang F, Zhang J, Lin X, Yang L, Zhou Q, Mi X, et al. METTL16 promotes translation and lung tumorigenesis by sequestering cytoplasmic eIF4E2. *Cell Rep*. 2023;42(3):112150.
15. Su R, Dong L, Li Y, Gao M, He PC, Liu W, et al. METTL16 exerts an m(6A)-independent function to facilitate translation and tumorigenesis. *Nat Cell Biol*. 2022;24(2):205–16.
16. Ruszkowska A. METTL16, Methyltransferase-Like Protein 16: Current Insights into Structure and Function. *Int J Mol Sci*. 2021;22:4.
17. Zhang H, Yin M, Huang H, Zhao G, Lu M. METTL16 in human diseases: what should we do next? *Open Med (Wars)*. 2023;18(1):20230856.
18. Monte M, Collavin L, Lazarevic D, Utrera R, Dragani TA, Schneider C. Cloning, chromosome mapping and functional characterization of a human homologue of murine gtse-1 (B99) gene. *Gene*. 2000;254(1–2):229–36.

19. Wang C, Xu J, Liu M, Liu J, Huang Y, Zhou L. [Relationship between GTSE1 and cell cycle and potential regulatory mechanisms in lung Cancer cells]. *Zhong-guo Fei Ai Za Zhi*. 2024;27(6):451–8.
20. El-Hussieny M, Thabet DM, Tawfik HM, Gayyed MF, Toni ND. The overexpression of NUSAP1 and GTSE1 could predict an unfavourable prognosis and shorter disease free survival in ccrenal cell carcinoma. *Asian Pac J Cancer Prev*. 2024;25(7):2551–9.
21. Zhang M, Wang X, Liu C, Zheng Z, Wan J, Yang Y, et al. G2 and S phase-expressed-1 induces chromosomal instability in esophageal squamous cell carcinoma cells and inhibits cell apoptosis through ROS/JNK signaling. *Mol Carcinog*. 2023;62(2):122–34.
22. Xie C, Xiang W, Shen H, Shen J. GTSE1 is possibly involved in the DNA damage repair and cisplatin resistance in osteosarcoma. *J Orthop Surg Res*. 2021;16(1):713.
23. Lin F, Xie YJ, Zhang XK, Huang TJ, Xu HF, Mei Y, et al. GTSE1 is involved in breast cancer progression in p53 mutation-dependent manner. *J Exp Clin Cancer Res*. 2019;38(1):152.
24. Yan G, Li J, Gao X, Liu J, Feng G, Li Y, et al. Comprehensive analysis of the diagnostic and therapeutic value, immune infiltration, and drug treatment mechanisms of GTSE1 in lung adenocarcinoma. *Front Med (Lausanne)*. 2024;11:1433601.
25. Yan G, Li G, Gao X, Liu J, Li Y, Li J, et al. GTSE1: A potential prognostic and diagnostic biomarker in various tumors including lung adenocarcinoma. *Clin Respir J*. 2024;18(5):e13757.
26. Yang X, Zhu X. G2 and S phase-expressed protein 1 is a biomarker for poor prognosis in lung adenocarcinoma. *Med (Baltim)*. 2024;103(12):e37358.

Publisher's note

Springer Nature remains neutral with regard to jurisdictional claims in published maps and institutional affiliations.